



# Voltage Control of Isolated Wind Energy Conversion System using Adaptive Voltage Controller for Non-Linear Loads

D Rajababu, K Raghu Ram

**Abstract:** Electrical energy demand increases day-by-day due to economic growth, technology development and increasing world population. The wind is one of the accessible renewable energy sources to generate electrical energy to meet the increased load demand. When the wind energy conversion system (WECS) is operating as isolated mode, it is more reliable, economical and easy to electrify rural areas. When the WECS is connected to load without controller the output three-phase voltages of the inverter have more transient and steady state errors and higher total harmonic distortion in the voltages and currents. This paper discusses various voltage controllers used in WECS in detail. The proposed WECS is simulated using MATLAB/Simulink with and without adaptive voltage controller for balanced and unbalanced non-linear load conditions. In each case the results have been analyzed and total harmonic distortion is evaluated..

**Keywords:** Adaptive Voltage Controller, Distributed Generation, and Total Harmonic Distortion, Wind Energy Conversion Systems.

## I. INTRODUCTION

Technology progression, economic growth and escalating population demand more and more electrical energy. To meet the load demand, usage of fossil fuels is increasing and may diminish in near future. When the electrical energy is generated from fossil fuels, they can release carbon gases and other wastages. Therefore, it leads to global warming and air pollution. The utilization of fossil fuels thereby resulting global warming can be reduced by generating the electrical energy from the renewable energy sources. The renewable energy sources like solar, wind, small hydro etc. are free available energy sources everywhere in the world. As compared with the conventional energy sources like coal, nuclear etc., the renewable energy sources are most environmental friendly [1]. The wind energy is one of the popular renewable energy sources and it is economically competent with the conventional energy sources [2]. The generation of electrical energy from the

wind energy is rapidly increases. In the year of 2018, new wind power plants installed capacity is 51.3 GW and total installed capacity reached 591 GW in the world. The Global Wind Energy Council (GWEC) expected that wind energy market is stable and every year new wind power plants installed capacity should be more than 50 GW up to 2023. The top ten wind power generating countries with the installed capacities (included onshore and offshore) at the end of 2018 shown in Table-I. India stands fourth position in wind power generation as shown in Fig. 1 [3].

**Table 1: Top ten wind generating countries with plant capacities**

S. No.	Name of the Country	Wind power plant capacity (MW)
1	China	23,000
2	USA	7,588
3	Germany	3,361
4	India	2,191
5	Brazil	1,939
6	UK	1902
7	France	1,563
8	Mexico	929
9	Sweden	717
10	Canada	566

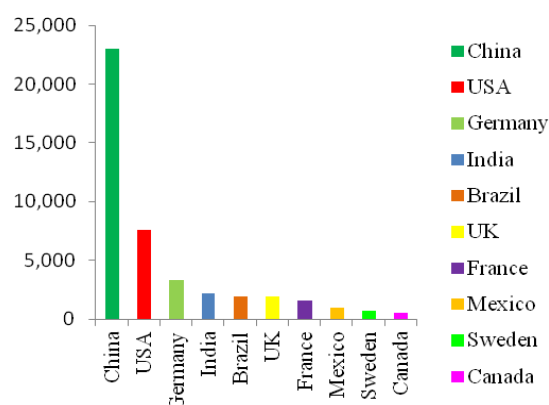


**Fig. 1. Top ten wind power generating countries with the respective generation capacities [3].**

The isolated wind energy conversion system (WECS) is required for electrification of rural villages, islands, ships and to meet the military requirements. The isolated power generation is often known as distributed generating systems (DGS). The advantages of DGS are:

Manuscript published on 30 September 2019

\* Correspondence Author

**D. Rajababu\***, EEE department, S R Engineering College, Warangal, India.

Email: durgamrajababu@gmail.com

**Dr. K. Raghu Ram**, EEE department, Laqshya Institute of Technology and Sciences, Khammam, India. Email: raghuramk00@gmail.com

© The Authors. Published by Blue Eyes Intelligence Engineering and Sciences Publication (BEIESP). This is an open access article under the CC-BY-NC-ND license <http://creativecommons.org/licenses/by-nc-nd/4.0/>

- Easy and fast installation because of the availability of prefabricated standardized components
- Reducing the installation cost by avoiding high voltage and long transmission lines
- The DGS with renewable energy sources is environmental friendly
- Operating cost is more or less constant
- Less dependability with simple construction, and consequent easy operation and maintenance
- Due to less complexity, there is a possibility of users participating as operators.

The functional diagram of the proposed isolated WECS is shown in Fig.1. The system has wind generator, an AC to DC rectifier, storage system, a DC to AC inverter, an inductive-capacitive filter and local load. The continuous lines shown in Fig. 1 represent the power flow and the dotted line represents the flow of sensor and control signals.

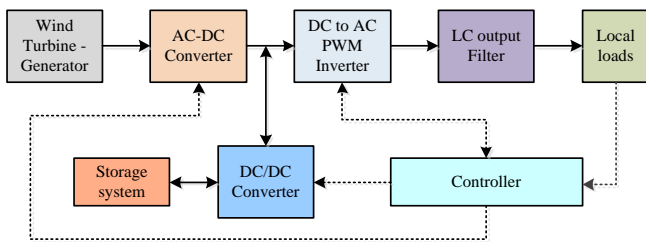


Fig. 2. Functional diagram of islanded wind power generation system.

## II. SYSTEM MODELING

The functional diagram shown in Fig. 3 consists of wind turbine coupled with the asynchronous alternator considered for the distributed power generation. The output from the considered DGS is alternating in nature which cannot be used in readily available format. Hence, it should be regulated and controlled before feeding the power to load. This could be achieved by using a rectifier circuit which could convert unregulated ac power into regulated dc power. The regulated dc power supply is considered as the integrated WES as given in the circuit diagram shown in Fig. 3. The circuit diagram includes a three-phase inverter connected to the non-linear load *via* an inductive and capacitive filter. The non-linear load contains a full-bridge rectifier connected to the resistive, inductive and capacitive elements. The mathematical modeling of the WECS shown in Fig. 3 is derived as given below.

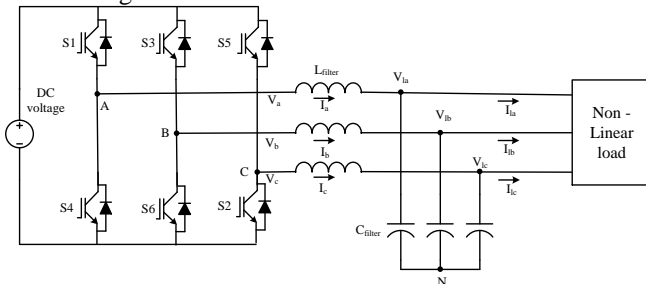


Fig. 3. Circuit schematic of the inverter connected to the non-linear load.

From the Fig.3, at the output terminals of the filter, according to Kirchhoff's voltage law and current law, the voltage and current equations can be represented as follows:

$$\frac{dV_l}{dt} = \frac{1}{C_{filter}} I - \frac{1}{C_{filter}} I_l \tag{1}$$

$$\frac{dI_l}{dt} = \frac{1}{L_{filter}} V - \frac{1}{L_{filter}} V_l \tag{2}$$

Where,  $I_s = [I_a \ I_b \ I_c]^T$ ,  $I_o = [I_{la} \ I_{lb} \ I_{lc}]^T$ ,

$V_s = [V_a \ V_b \ V_c]^T$ ,  $V_o = [V_{la} \ V_{lb} \ V_{lc}]^T$ ,  $C_{filter}$  is the per phase capacitance of filter, and  $L_{filter}$  is the per phase inductance of filter.

The 3- $\phi$  stationary a-b-c reference frame equations given in (1) and (2) can be transformed into stationary  $\alpha$ - $\beta$  reference frame as given in (3) and (4). Then, the stationary  $\alpha$ - $\beta$  reference frame equations are converted into synchronously rotating d-q reference frame.

$$\frac{dV_{l\alpha\beta}}{dt} = \frac{1}{C_{filter}} I_{\alpha\beta} - \frac{1}{C_{filter}} I_{l\alpha\beta} \tag{3}$$

$$\frac{dI_{l\alpha\beta}}{dt} = \frac{1}{L_{filter}} V_{\alpha\beta} - \frac{1}{L_{filter}} V_{l\alpha\beta} \tag{4}$$

where,  $V_{l\alpha\beta} = [V_{l\alpha} \ V_{l\beta}]^T$ ,  $I_{l\alpha\beta} = [I_{l\alpha} \ I_{l\beta}]^T$

$$V_{\alpha\beta} = [V_{\alpha} \ V_{\beta}]^T, I_{\alpha\beta} = [I_{\alpha} \ I_{\beta}]^T$$

$$\frac{dV_{ldq}}{dt} + j\omega V_{ldq} = \frac{1}{C_{filter}} I_{\alpha\beta} - \frac{1}{C_{filter}} I_{l\alpha\beta} \tag{5}$$

$$\frac{dI_{dq}}{dt} + j\omega I_{dq} = \frac{1}{L_{filter}} V_{\alpha\beta} - \frac{1}{L_{filter}} V_{l\alpha\beta} \tag{6}$$

where,  $V_{ldq} = [V_{ld} \ V_{lq}]^T$ ,  $I_{ldq} = [I_{ld} \ I_{lq}]^T$

$$V_{dq} = [V_d \ V_q]^T, I_{dq} = [I_d \ I_q]^T$$

## III. VOLTAGE CONTROL TECHNIQUES

As per the literature survey [4]-[10], the 3- $\phi$  inverter (shown in Fig.3) output voltages and currents can be controlled by different control strategies when it is connected to various loads fed from renewable energy sources. Some of the control strategies includes proportional and integral controller, flatness based controller and adaptive controller. A brief explanation is given in the following sub-sections about these controllers.

**1. Proportional and Integral Controller:**

The load side voltage and frequency of the system shown in Fig. 3 can also be controlled by vector control technique as shown in Fig. 4. The conventional proportional and integral (PI) controller is used for compensating the error signal which is the difference between the measured and reference signals. Three PI controllers are used viz two voltage controllers in outer loop and one current controller in the inner loop. In voltage control loop, measured voltage is compared with the reference voltage. The resultant value of one of the outer voltage loop is compared with the output of the inner current loop of the DC link voltage controller. The PI controller is used to regulate the error whereas a phase lock loop (PLL) is used for the reference frequency [4].

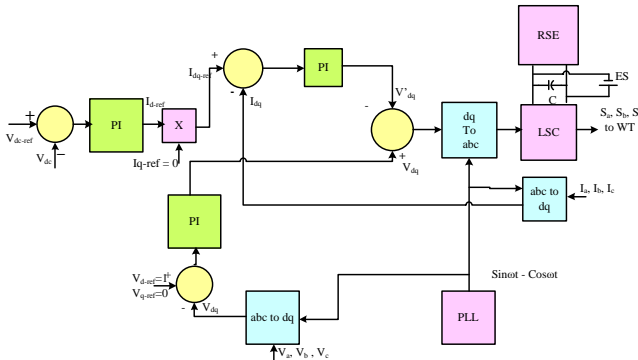


**Fig. 4. Proportional and integral controllers for load side converter.**

The compensated signal is determined by the equation:

$$C_{sig} = k_p \Delta e + \int k_i \Delta e \quad (7)$$

Where,  $k_p$  and  $k_i$  are proportional and integral constants of PI controller.

$\Delta e$  is the difference between reference and measured signal.

In isolated power distribution system, the load side voltage is controlled by PI controller by compensating the voltage error. The controller is also used to control the frequency within the limits. In case of over voltage generation, the energy stored in the storage system and dummy load is connected to maintain the frequency within the limits. Similarly under voltage generation, storage system injects the power to maintain the frequency within the limits. The usage of dummy load will lead to the excess power loss in the system.

**2. Flatness Based Control:**

The flatness based control (FBC) is one of the good control schemes used to operate three-phase inverters, especially in isolated mode of renewable energy system operation. The main object of differential flatness control method is to observe the system state variables during steady state and transient state. Therefore dynamic response of the system and improved behavior of the system at different types of loads is obtained by one-loop control method. The control structure consists of an electrostatic energy loop which allows ensuring the creation of a three-phase voltage network with the desired magnitude and frequency and those with a low harmonic distortion rate. The use of only one control loop allows obtaining high dynamic properties of the system which

ensure small harmonic distortion rate of the output voltage [5].

The following equations can be used to design the flatness based controller as shown in Fig. 5.

$$(\gamma_d - \ddot{y}_{d-ref}) + k_1(\dot{y}_{d-ref} - \dot{\gamma}_d) + k_2(y_{d-ref} - \gamma_d) + k_3 \int (y_{d-ref} - \gamma_d) d\tau = 0 \quad (8)$$

$$(\gamma_q - \ddot{y}_{q-ref}) + k_1(\dot{y}_{q-ref} - \dot{\gamma}_q) + k_2(y_{q-ref} - \gamma_q) + k_3 \int (y_{q-ref} - \gamma_q) d\tau = 0 \quad (9)$$

$$\begin{pmatrix} V_{d-ref} \\ V_{q-ref} \end{pmatrix} = \phi(\gamma_{d-ref}, \dot{\gamma}_{d-ref}, \gamma_d, \gamma_{q-ref}, \dot{\gamma}_{q-ref}, \gamma_q) \quad (10)$$

$$y_{d-ref-f} = \frac{1}{2} C_{filter} V_{cd-ref}^2 \left( 1 - e^{-\frac{t-t_{init}}{\tau_1}} - \frac{t-t_{init}}{\tau_1} e^{-\frac{t-t_{init}}{\tau_1}} \right) \quad (11)$$

$$y_{q-ref-f} = \frac{1}{2} C_{filter} V_{cq-ref}^2 \left( 1 - e^{-\frac{t-t_{init}}{\tau_1}} - \frac{t-t_{init}}{\tau_1} e^{-\frac{t-t_{init}}{\tau_1}} \right) \quad (12)$$

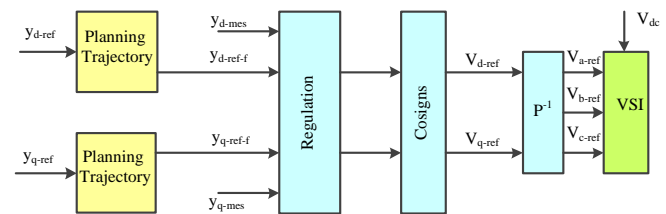


**Fig. 5: Operational diagram of the flatness based controller.**

In the flat controllers to reduce the noise effects, the reference reactions are used instead of disturbance reactions. This approach helps in foreseeing the transients analytically which is not possible using the other classical approaches. Here, the linearization of feedback through I/Os eliminates the dynamic zeros. In addition, this controller uses less number of sensors.

The flatness based controller results in lower voltage THDs, higher dynamic performance, safety start-up, and better performance against variations in the system parameters. However, this method is complex and need high computing processors.

**3. Adaptive voltage control:**

The reference adaptive control theory can be used to design the adaptive voltage controller [6]. The voltage controller performance can be decided by the reference parameters. The reference parameters considered for the controller are inverter output voltages sensed before and after the filter, inverter or load currents. The values of inverter output or load currents are crucial in the considered system, because of the non-linear load. These sensed parameters are compared with the reference parameters and the error signal is generated which is compensated using below given procedure.

The compensation and the feedback control parameters say

$u_{cd}$  &  $u_{cq}$  and  $u_{fd}$  &  $u_{fq}$  respectively are used as adaptive control laws for the considered WECS. These control parameters can be represented in terms of adaptive gains  $m_{id}$  and  $m_{iq}$ .

$$u_{cd} = \sum_{i=1}^4 m_{di} P_{di} + V_{ld}, u_{fd} = -\partial_d \sigma_d \quad (13)$$

$$u_{cq} = \sum_{m=1}^4 m_{qi} P_{qi} + V_{lq}, u_{fq} = -\partial_q \sigma_q \quad (14)$$

The adaptive gains  $m_{id}$  and  $m_{iq}$  can be defined as follows:

$$m_{id} = -\frac{1}{\phi_{di}} \int_0^t P_{di} \sigma_d d\tau \quad (15)$$

$$m_{iq} = -\frac{1}{\phi_{qi}} \int_0^t P_{qi} \sigma_q d\tau \quad (16)$$

And the functions  $\sigma_d$  and  $\sigma_q$  can be defined as:

$$\sigma_d = \bar{V}_{ld} + \alpha_d \bar{I}_{id} \quad (17)$$

$$\sigma_q = \bar{V}_{lq} + \alpha_q \bar{I}_{iq} \quad (18)$$

where,  $\alpha_d$  and  $\alpha_q$  are positive design constants,  $m_{id}$  and  $m_{iq}$  are the estimated values for  $m_{id}^*$  and  $m_{iq}^*$ ,  $\delta_d$  is greater than 0,  $\delta_q$  is greater than 0,  $\phi_{di}$  is greater than 0, and  $\phi_{qi}$  is greater than 0.

The adaptive gains given in equations (15) and (16) can be tuned to larger values so as to realize the quicker convergence and better transient response. Hence, the values selected for  $\phi_{di}$  and  $\phi_{qi}$  must be smaller values as per the relation between adaptive gains and  $\phi_{di}$  and  $\phi_{qi}$  which is inverse relation. In addition, the control parameters  $\alpha_d$ ,  $\alpha_q$ ,  $\delta_d$ , and  $\delta_q$  can be calculated with respect to the tuning rule. All the above mentioned parameters are calculated as shown in Fig. 6. These calculations are continued till the desired transient response is obtained and the solution is converged.

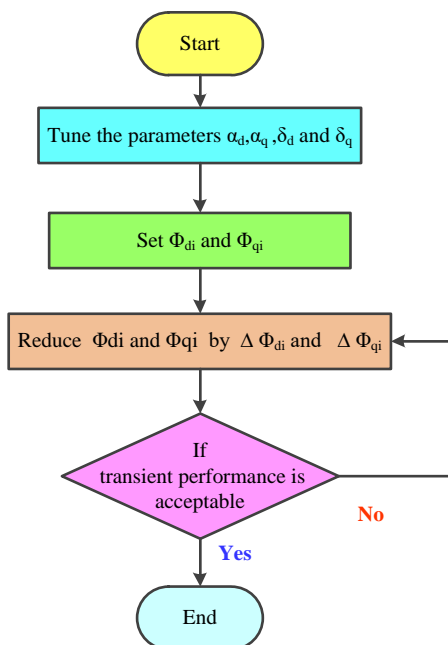


Fig.6: Flow chart of operation of the adaptive controller

#### IV. DISCUSSION ON SIMULATION RESULTS

The proposed isolated WECS is simulated with and without adaptive voltage controller for balanced and unbalanced non-linear loads using MATLAB/Simulink. The simulation results of the system are shown in Fig. 6 to 9. The system parameters which are using in the simulation are shown in appendix.

##### A. Balanced non-linear load:

Fig. 7 shows the simulation results of the system shown in Fig. 2 for balanced conditions of RL-load without using the controller. The simulation results include (from top to bottom) three-phase load voltages ( $V_{labc}$ ), three-phase load currents ( $I_{labc}$ ), input side dq-axis voltages ( $V_{sdq}$ ), three-phase source currents ( $I_{sabc}$ ) and controller currents transformed from dqo to abc reference frame ( $I_{tran}$ ). Initially the circuit breaker is kept open and at time  $t=0.1$  seconds the circuit breaker is closed. From the results, it can be observed that the load side voltage and current variations are more and they are not sinusoidal waveforms. The load current is zero from time 0 to 0.1 seconds which is because of the circuit breaker setting. The source current waveforms also show non-sinusoidal behavior because of the absence of controller. Also, the controller currents,  $I_{trans}$  are zero which depicts the absence of controller. The total harmonic distortion (THD) of one of the phase current is obtained from the simulation results and is about 190.01%.

The simulation results of wind energy conversion system (see Fig. 2) with balanced non-linear load, without controller are shown in Fig. 6. The results consists of 3- $\phi$  load voltages, 3- $\phi$  load currents, input side direct and quadrature axis voltages, 3- $\phi$  source currents and the controller currents transformed from dqo to abc reference frame. Before switching the circuit breaker is kept open and time at  $t=0.1$  seconds the circuit breaker is closed. From the Fig. 6, it can be observed that without controller the non-linear load side voltage and current variations are more. The load side phase-a, phase-b and phase-c currents total harmonic distortion (THD) is obtained as 249.85%, 240.03% and 154.9% respectively. From the values of THDs it can be concluded that all the phase currents are unequal and thus result in unequal THD values, which is undesirable for non-linear loads as well as for linear loads.

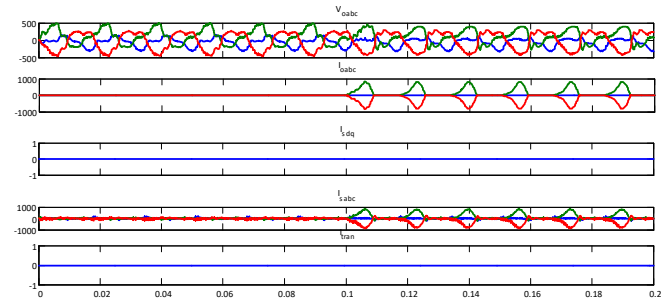
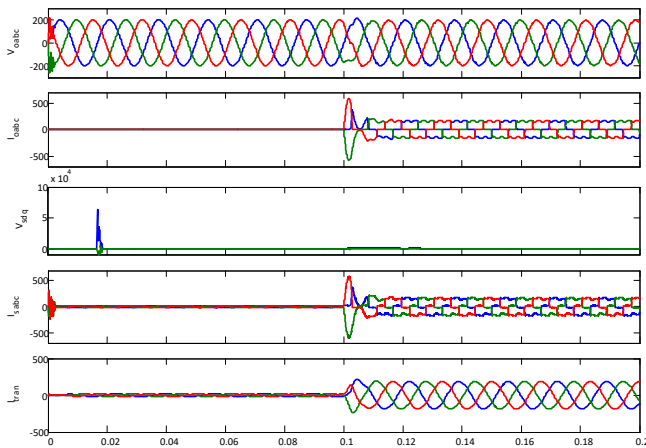


Fig. 7: Results showing the operation of system without using the controller for balanced non-linear load.

The simulation results of the wind energy conversion system with non-linear balanced load and using adaptive controller are shown in Fig. 8. From the results it is observed that the three-phase load voltages are pure sinusoidal

and balanced, which confirms the working of adaptive voltage controller. After switching the circuit breaker (at  $t=0.1$  seconds, circuit breaker can be closed), the load side current has the percentage of THD is 31.12% and is equal in all the phases.



**Fig. 8: Results showing the operation of system with the adaptive controller for balanced non-linear load.**

**B. Unbalanced non-linear load:**

The same system which is shown in Fig. 2 with non-linear unbalanced load without using any controller is simulated. The simulation results are shown in Fig. 9. Here, phase-a is considered as faulty phase for creating unbalance condition between three-phases (circuit breaker of phase-a is opened at time  $t = 0.1$  seconds). From the results, it is observed that the load side three-phase voltages and unbalanced currents are non sinusoidal. The total percentage of THD for phase-b and phase-c are obtained as 232.15%, whereas phase-a current is zero and hence no THD.

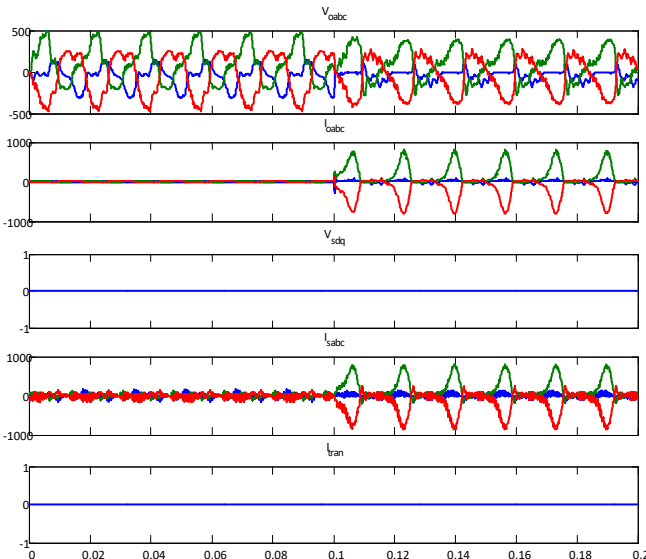


**Fig. 9: Results showing the operation of system without controller for unbalanced non-linear load.**

Further, the same system is simulated with adaptive voltage controller for unbalanced non-linear load conditions as shown in Fig. 2. In this case also phase-a is considered as faulty phase (circuit breaker phase-a is opened at  $t=0.1$  sec). The simulation results are shown in the Fig. 10. In this case, even though the system is unbalanced and fed to the

non-linear load the three-phase voltages are controlled to be sinusoidal, which is because of the adaptive voltage controller. The percentage THD of the remaining healthy phase currents is obtained as 54.64% and is equal for both the phases-b and c.

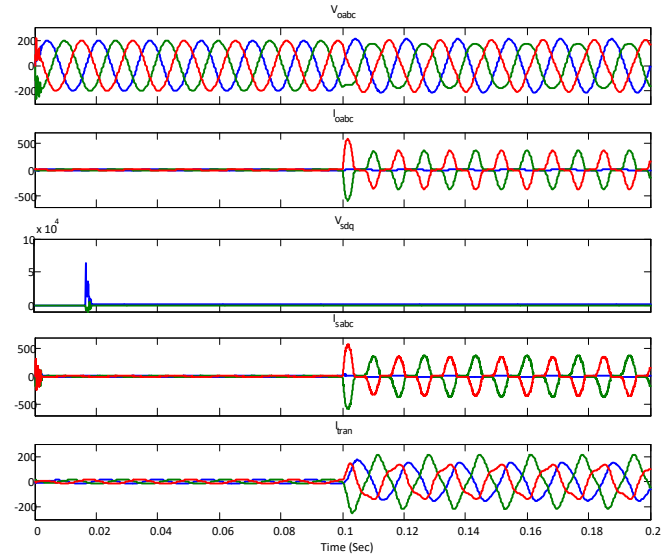


**Fig. 10: Results showing the operation of system with the adaptive controller for unbalanced non-linear load.**

**V. CONCLUSION**

In this manuscript, an isolated wind energy conversion system is considered and is studied for various loading conditions. The WECS is operated using an adaptive voltage controller which uses the sensed data from the dc-bus, load and the filter. The sensed parameters are then processed and the required voltage and current waveforms are generated so as to feed the power to the non-linear load, which is considered to be critical in any isolated and non-isolated renewable energy systems. The performance of the controller is validated for balanced and unbalanced kinds of loads. The simulation results shown in this manuscript, depicts the effective working of the adaptive voltage controller for both the balanced and unbalanced non-linear load conditions.

**APPENDIX**

- DC Supply Voltage ( $V_{DC}$ ) = 564Volts
- Filter Inductance ( $L_{filter}$ ) = 0.3 mH
- Filter Capacitance ( $C_{filter}$ ) = 500  $\mu$ F
- Inverter Output frequency ( $f$ ) = 50Hz
- Non-linear load: Full-bridge diode rectifier connected to Resistor( $R$ ) = 1.2 Ohms, Inductor( $L$ ) =  $0.3e^{-3}$ H, and Capacitor( $C$ ) = 4000 $\mu$ F load.

**REFERENCES**

1. Gil D. Marques and Matteo F. Iacchetti, "Sensorless Frequency and Voltage Control in the Stand-Alone DFIG-DC System", IEEE Transactions on Industrial Electronics, Vol. 64, No. 3, pp.1949-1957, March 2017.
2. Akhila Gundavarapu, Himanshu Misra, and Amit Kumar Jain , "Direct Torque Control Scheme for DC Voltage Regulation of the Standalone DFIG-DC System", IEEE Transactions on Industrial Electronics, Vol. 64, No. 5, pp. 3502 3211, May 2017.
3. <https://www.compositesworld.com/news/gwec-reports-513-gw-of-new-wind-capacity-in-2018>



4. M. Aktarujjaman, M.A. Kashem, M. Negnevitsky, and G. Ledwich, "Control Stabilization of an Isolated System with DFIG Wind Turbine", First International Power and Energy Conference PECON 2006, pp.313-317, November 28-29, 2006.
5. Azeddine Houari, Hugues Renaudineau, Jean-Philippe Martin, Serge Pierfederici, and Farid Meibody-Tabar, "Flatness-Based Control of Three-Phase Inverter With Output LC Filter", IEEE Transactions on Industrial Electronics, Vol. 59, No. 7, pp. 2890- 2897, July 2012.
6. Ton Duc Do, Viet Quoc Leu, Young-Sik Choi, Han Ho Choi, and Jin-Woo Jung, "An Adaptive Voltage Control Strategy of Three-Phase Inverter for Stand-Alone Distributed Generation Systems" IEEE Transactions on Industrial Electronics, Vol. 60, No. 12, pp. 5660-5672, December 2013.
7. Giuseppe Fusco and Mario Russo, "Adaptive Voltage Control in Power Systems Modelling, Design and Applications" Advances in Industrial Control series ISSN 1430-9491© Springer-Verlag London Limited 2007.
8. A. M. Kassem, A. A. Hassan and Yehia S. Mohamed, "Adaptive Voltage and frequency Control of an Isolated Wind-Generation System Using Neural Networks" 4th Saudi Technology Conference and Exhibition (STCEX06), Riyadh, Saudi, pp. 2-6, 2006.
9. Daniel G. Forchetti, Guillermo O. Garcia, María Inés Valla, "Adaptive Observer for Sensorless Control of Stand-Alone Doubly Fed Induction Generator", IEEE Transactions On Industrial Electronics, Vol. 56, No. 10, pp:4174-4180, OCTOBER 2009
10. Dr. B. Rajender, B. Sathyavani, K. Balakrishna, Dr. R. Arulmurugan "An Overview of Microprocessor Control of Inverters" International Journal of Engineering & Technology, volume 7 , Issue 3.24, pp:532-535, December 2018.

## ACKNOWLEDGMENT

The author would like to thanks to the Management and the Head, Centre for Emerging Energy Technologies, S R Engineering College, Warangal, for supporting to publish this paper.

## AUTHORS PROFILE



**Mr.D.Rajababu**, received B. Tech. degree in Electrical and Electronics Engineering in 1999 from Jawaharlal Nehru Technological University College of Engineering, Ananthapuram, Andrapradesh and M. Tech. in Electrical Power Systems in 2002 from the same college. He is presently pursuing Ph.D from the Jawaharlal Nehru Technological University, Hyderabad. His

interested areas are Power system analysis and renewable energy sources.



**Dr. K. Raghu Ram**, received B. Tech degree in Electrical and Electronics Engineering in 1979 from Jawaharlal Nehru Technological University College of Engineering, Hyderabad, M. Tech. in Electrical Power Systems in 1983 from the same college. He received Ph.D. from Jawaharlal Nehru Technological University College of Engineering,

Hyderabad in the year of 2004. His interested areas are stability analysis of three- phase to six-phase interconnected systems and renewable energy sources.